PCCP

Visualization of the effective potential and Coulomb correlations in finite metallic systems

F. Despa and R. S. Berry

Department of Chemistry, The University of Chicago, Chicago, Illinois 60637, USA

Received 13th December 2001, Accepted 16th April 2002
First published as an Advance Article on the web 14th June 2002

We present an analytic *ansatz* to find the effective electrostatic potential and Coulomb correlations in multicenter problems, specifically homogeneous and doped clusters of metal atoms. The approach is based on a quasi-classical density-functional treatment. We focus on the interpretive aspect of our findings, particularly on extracting insight regarding the geometric effects of Coulomb correlations for any given spatial disposition of ionic cores. For singly-doped metallic clusters we obtain a direct visualization of the variations of both screening and Coulomb correlations with changes of location of the dopant atom. This analysis provides a way to interpret recent observations of the variability of physical properties of metal clusters with changes of composition and geometry.

Perception in terms of concepts that can be visualized is an important part of understanding physical phenomena. Presently, such an interpretative theoretical tool may provide a valuable way of guiding the analysis of experiment in the realm of atomic clusters. Hence, we develop an analytic approach that makes it possible to find and visualize the effective electrostatic potential and Coulomb correlations in multicenter problems. We make use of the quasi-classical density-functional theory to account for the electron self-distribution in the common cluster potential. While this is not at the same level of studies of electron correlations in atoms, for which very accurate wave functions have been used, it is a significant step beyond the "jellium" model, frequently-invoked in describing moderately large metallic clusters.[1]

Collective effects induced by Coulomb correlations in atoms have been studied in two ways. In the first, both hydrodynamic theory and local approximate dielectric theory have been used; neither of these takes into account either shell structure or the single-particle spectrum of the valence electrons.[2] These methods are capable, at most, of giving gross trends in dynamical properties. The second route instead uses a fully quantal description based on the one-electron excitation spectrum and corresponding wavefunctions. A recent collection of papers provides a description of methods and results of the application of many-body techniques in atomic theory.[3]

The way electrons are correlated can be inferred from the probability distribution implied by their wavefunction.[4] To make such inferences, however, we must be a bit thoughtful about how we present this distribution. Even for a two-electron atom, we begin with a function of six independent variables in a fixed-center-of-mass system. We would like to extract from this a description in no more than two or three independent variables, something we can represent pictorially and visualize.

For a three-body system such as He** or the valence electrons of Mg, a natural and practical way to carry out such a description has emerged as an analytic reduction of the probability density $|\Psi(\boldsymbol{r}_1,\boldsymbol{r}_2)|^2$ to the joint probability density $p(r_1,r_2,\theta_{12})$, where θ_{12} is the angle between the position vectors r_1 and r_2 of two electrons.[5,6] This in turn makes it straightforward to compute and display the conditional probability density $d(r_2,\theta_{12};r_1)$ for finding one of the two electrons at distance r_1 from the nucleus, and at an angle θ_{12} from the vector from the nucleus to electron 2 if electron 2 is at a distance r_2 from the nucleus.

Three-dimensional graphs of $d(r_1,r_2,\theta_{12})$ provide a vivid and precise way to depict the correlation of two electrons.[7] With this probability density d, one can compare wavefunctions of different qualities, see what roles long-range and short-range correlation play in various states, exhibit the relative importance of angular and radial correlation, and compare correlation in different atomic systems. The work, started in the late 1970s by Rehmus, Kellman, Roothaan and Berry,[5,6] provides a generalization of other quantitative descriptions of electron correlation.[8–16] At this point, reference must be made to the important progress in studying the correlation effects in atoms and molecules that followed from the two-particle density-matrix approach,[17] d-dimensional theory,[18–20] the coupled-cluster method,[21–23] and the density-functional approach.[24–26]

For a system of more particles, we have yet to find a comparably powerful approach because so much information is contained in the wave function and we do not know how to extract what is relevant in a manner adaptable to pictures. An exception emerges, obviously, for the high-density limit of the Fermi fluid where a collective description of electrons is likely to be optimal. This collective description is based on the organized behavior of the electrons brought about by their long-range Coulomb interactions. The long-range Coulomb interactions, subject to screening by the other electric charges, act to couple together the motion of many electrons, giving rise to the well-known quantum density or plasmon oscillations.[27]

Working toward extracting insights from the probability density $|\Psi|^2$ and making use of the quasi-classical description for the (valence) electron gas, we develop here an analytical *ansatz* which allows us to find and visualize the effective electrostatic potential and Coulomb correlations in multicenter problems. We apply this *ansatz* to the case of moderately large metallic clusters. To anticipate what follows, let us state our findings: by using a generalized partition function for valence electrons (the Bloch density matrix), the electron self-distribution in the common potential $V(\boldsymbol{r})$ is derived in terms of many-body perturbation theory.[28] This approach produces the electron density $\rho(\boldsymbol{r})$ as a functional of $V(\boldsymbol{r})$ (with $\rho(\boldsymbol{r})\sim V(\boldsymbol{r})$), which is valid for describing metallic systems, *i.e.* systems with a high-density valence electron gas. Further, inside the electron

 DOI: 10.1039/b111394c

gas of density $\rho(\boldsymbol{r})$, we introduce the cluster cage formed by the positive ion cores with the spatial distribution given by $\rho_+(\boldsymbol{R}_i)$, and apply Poisson's equation to the cluster as a whole. (The vectors $\boldsymbol{R}_i$ are position vectors of the ions.)

The self-consistent solution of this equation gives the collective description of the cluster constituents, electrons plus ions. This generalization of the Coulomb interaction results in a superposition of quantum oscillations given by long-range contributions and screening on the smooth "semiclassical" potential.[29] We focus on their interpretive aspects and specifically on extracting insights regarding the geometric effects of Coulomb correlations for any given spatial disposition of ionic cores. Also, we explore the case of a foreign metal atom doping an otherwise-homogeneous cluster of metal atoms. The approach presented here provides us with a direct visualization of the way both the screening effect and the Coulomb correlations change with changes of the location of the impurity. This analysis is important in the context of recent observations of the role played by composition and geometry in changing the physical properties of metallic clusters.[30–32]

Consider a fixed positive ion distribution in space $\rho_+(\boldsymbol{R}_i)$, with $\boldsymbol{R}_i$ the positions of the ions measured from the center of the cluster. The ion cluster cage has a net charge measured in appropriate units equal to zN, where z is the electric charge of one ion (for simplicity, we shall restrict the discussion to single-valent metals, $z = 1$) and N denotes the total number of ions in the cluster. If a gas of valence electrons carrying an equal number of negative charges is introduced, so that the system is strictly neutral, then the electrons redistribute themselves so as to shield the positive charges at large distances and minimize the Coulomb self-energy of that gas, and also satisfy the fermion constraints on the electrons. In the high density limit of the Fermi fluid, Bohr's correspondence principle applies and we can introduce the collective description of the electron gas based on the methods of statistical mechanics. The generalized partition function of the valence electrons moving in the common potential $V(\boldsymbol{r})$ can be written in terms of the wavefunctions $\Psi_i(\boldsymbol{r})$ and energy levels ε_i as

$$\Gamma(\boldsymbol{r}', \boldsymbol{r}, \beta) = \sum_i \Psi_i^*(\boldsymbol{r}')\Psi_i(\boldsymbol{r})\mathrm{e}^{-\varepsilon_i\beta}, \tag{1}$$

where $\beta = (k_\mathrm{B}T)^{-1}$, k_B is Boltzmann's constant and T the absolute temperature. By integrating this along the diagonal, where $\boldsymbol{r}' = \boldsymbol{r}$, we obtain the ordinary partition function of statistical mechanics. Eqn. (1) is the Bloch density matrix and if we operate with the one-particle Hamiltonian

$$H_\mathrm{s} = -\frac{1}{2}\nabla_r^2 + V(\boldsymbol{r}), \tag{2}$$

on Γ, and compare the result with that obtained by differentiating Γ with respect to β, then we find the Bloch equation

$$H_\mathrm{s}\Gamma = -\frac{\partial\Gamma}{\partial\beta}, \tag{3}$$

which has the form of the time-dependent Schrödinger equation, with β playing the role of it. The boundary condition required to define the solution of eqn. (3) follows from the completeness theorem for eigenfunctions, namely

$$\Gamma(\boldsymbol{r}', \boldsymbol{r}, 0) = \delta(\boldsymbol{r}' - \boldsymbol{r}).$$

In the high density limit, the behavior of the electrons is simple, and the Coulomb interaction can be treated as a perturbation of the motion of the free electrons. Therefore the solution of eqn. (3) may be written as

$$\Gamma(\boldsymbol{r}', \boldsymbol{r}, \beta) = \Gamma_0(\boldsymbol{r}', \boldsymbol{r}, \beta) - \int \mathrm{d}\boldsymbol{r}'' \times \int_0^\beta \mathrm{d}\beta'\, \Gamma_0(\boldsymbol{r}', \boldsymbol{r}'', \beta - \beta')V(\boldsymbol{r}'')\Gamma(\boldsymbol{r}'', \boldsymbol{r}, \beta'), \tag{4}$$

where Γ_0 is the Bloch density matrix for an assembly of free electrons. The derivation of Dirac's density matrix $\gamma(\boldsymbol{r}',\boldsymbol{r})$ from eqn. (4) is described in ref. 28. It consists of an iterative procedure to find the perturbation terms in Γ. The first step is the replacement of Γ_0 for Γ in the integral and integration over β'. If the Bloch density matrix Γ is determined, Dirac's density matrix γ (which is actually the electron density) may be obtained by using the Laplace transform relation connecting $\Gamma(\boldsymbol{r}',\boldsymbol{r},\beta)$ and $\gamma(\boldsymbol{r}',\boldsymbol{r},\xi)$

$$\Gamma(\boldsymbol{r}', \boldsymbol{r}, \beta) = \beta\int_0^\infty \mathrm{d}\xi\, \gamma(\boldsymbol{r}', \boldsymbol{r}, \xi)\exp(-\beta\xi),$$

where ξ is an intensive energy variable conjugate to β.

Following the above procedure, the electron density is obtained as

$$\rho(\boldsymbol{r}) = \rho_0 - \frac{k_\mathrm{F}^2}{2\pi^3}\int \mathrm{d}\boldsymbol{r}'\, V(\boldsymbol{r}')\,\frac{j_1(2k_\mathrm{F}|\boldsymbol{r} - \boldsymbol{r}'|)}{|\boldsymbol{r} - \boldsymbol{r}'|^2}. \tag{5}$$

Here k_F is the Fermi wavevector, ρ_0 is the free-particle density, $\rho_0 = k_\mathrm{F}^3/(3\pi^2)$, and $j_1(x)$ is the first-order spherical Bessel function.

With the primary form eqn. (5), the electron density $\rho(\boldsymbol{r})$ makes further mathematical computations very difficult. To go further, we need to simplify by linearizing. Usually, this linearization proceeds by adding the assumption that $V(\boldsymbol{r})$ varies slowly in space, the Thomas–Fermi approximation. Accordingly, $V(\boldsymbol{r}')$ is replaced in eqn. (5) by $V(\boldsymbol{r})$.[33] One obvious point needs to be stressed here: the discrete positive ion distribution used here produces a Coulomb potential with a far more structured (and realistic) spatial variation than that of the frequently-invoked continuum distribution of the "jellium" models.[1] The linearization in eqn. (5) can still be made under the following assumptions. Our main observation at the outset is that in a high-density electron gas, any electric charge is screened out very rapidly, namely, at distances beyond a characteristic Debye screening length, say q_0^{-1} (which is inversely proportional to $\sqrt{k_\mathrm{F}}$, as can be seen below). Also, we notice that the slow variation of $V(\boldsymbol{r})$ is usually supposed to be over a de Broglie wavelength for an electron at the Fermi surface, that is $2\pi/k_\mathrm{F}$. From this view, we may say that a possible conflict with the use of the Thomas–Fermi approximation occurs only close to the positive ions, closer than a shielding distance q_0^{-1}. Disregarding this limitation, we use the Thomas–Fermi approximation in eqn. (5) to obtain, after a straightforward integration,[28]

$$\rho(\boldsymbol{r}) = \rho_0 - \frac{q_0^2}{4\pi}V(\boldsymbol{r}), \tag{6}$$

where $q_0^2 = 4k_\mathrm{F}/\pi a_0$, with a_0 the Bohr radius. The results are not strongly affected by this approximation. For example, good agreement within natural limits has been obtained previously[34] for the fullerene molecule described in this way and without the simplifying linearization. At the same time, we can see that the density follows the potential closely, which means that the validity of the theory is ensured, as we already stipulated above, by an appropriate requirement on the electron density. Of course this approximate theoretical model loses its validity at large distances from the ion locations because the electron density vanishes, and at very short distances, towards the center of the cluster cage, where the density becomes infinite with the potential.[35]

Eqn. (6) is a quasi-classical result obtained in the high density approximation for the valence electrons. Within the quasi-classical approximation,[36] local variations of the electron density leave the exchange contribution unchanged, as a consequence of its nonlocal (quantum) character. Therefore, a first-order quantum correction to this quasi-classical result

represents the exchange energy

$$E_{\mathrm{ex}} = -\frac{3}{4}\left(\frac{3}{\pi}\right)^{1/3}\rho_0^{4/3},$$

Consequently, we may assume that the common potential $V(\boldsymbol{r})$ is generated only by the electron distribution in the presence of the discrete ionic background. We may therefore set up the basic Poisson equation to yield

$$\Delta V = 4\pi\rho_0 - q_0^2 V(\boldsymbol{r}) - 4\pi\sum_i^N z_i\delta(\boldsymbol{r}-\boldsymbol{R}_i). \quad (7)$$

We have to solve a self-consistent field problem which accounts for the electron distribution profile in the presence of a discrete positive background. The last term on the right side of eqn. (7) represents the density of positive charge with R_i the average distance of an ion from the center of the cluster and i is an index running over the ions, each with electric charge z_i. These locations are chosen without regard to the stability of the configuration.

According to the principle of superposition, Poisson's equation, eqn. (7), may separate:

$$\Delta(V_1+V_2) = 4\pi\rho_0 - q_0^2 V_1 - q_0^2 V_2 - 4\pi\sum_{i=1}^N z_i\delta(\boldsymbol{r}-\boldsymbol{R}_i), \quad (8)$$

which means that we have to solve two simpler equations rather than one very complex equation. The first is given by

$$\Delta V_1 = 4\pi\rho_0 - q_0^2 V_1, \quad (9)$$

and represents the effective electrostatic potential due to the electron self-distribution where the discrete nature of the positive charges is disregarded. This equation will be solved inside a large sphere of radius R, which has to contain most of the valence electron density.[37] The second equation becomes

$$\Delta V_2 = -q_0^2 V_2 - 4\pi\sum_{i=1}^N z_i\delta(\boldsymbol{r}-\boldsymbol{R}_i), \quad (10)$$

and accounts for the remaining terms of the total potential. The discrete nature of the positive background is employed here.

By Fourier transformation, the latter equation becomes

$$\int \mathrm{d}\boldsymbol{k}\; V_2(k)(k^2-q_0^2)\exp(\mathrm{i}\boldsymbol{k}\boldsymbol{r}) = \frac{1}{2\pi^2}\sum_{i=1}^N z_i\int \mathrm{d}\boldsymbol{k}\exp[\mathrm{i}\boldsymbol{k}(\boldsymbol{r}-\boldsymbol{R}_i)], \quad (11)$$

wherefrom

$$V_2(k) = \frac{1}{2\pi^2}\sum_{i=1}^N z_i\frac{\exp(-i\boldsymbol{k}\boldsymbol{R}_i)}{k^2-q_0^2},$$

and the potential is simply

$$V_2(\boldsymbol{r}) = \frac{1}{2\pi^2}\sum_{i=1}^N z_i\int \mathrm{d}\boldsymbol{k}\frac{\exp[\mathrm{i}\boldsymbol{k}(\boldsymbol{r}-\boldsymbol{R}_i)]}{k^2-q_0^2}, \quad (12)$$

or

$$V_2(\boldsymbol{r}) = \frac{2}{\pi}\sum_{i=1}^N z_i\sum_{lm} i^l\int \mathrm{d}k\frac{k^2}{k^2-q_0^2}j_l(k|\boldsymbol{r}-\boldsymbol{R}_i|) \times \int \mathrm{d}\Omega_k\, Y_{lm}^*(\theta_k,\varphi_k)\; Y_{lm}(\theta_i,\varphi_i),$$

in terms of spherical Bessel functions $j_l(k|\boldsymbol{r}-\boldsymbol{R}_i|)$. After the integration over Ω_k, the above equation for the potential reduces to

$$V_2(\boldsymbol{r}) = \frac{2}{\pi}\sum_{i=1}^N z_i\int \mathrm{d}k\frac{k^2}{k^2-q_0^2}\sin(k|\boldsymbol{r}-\boldsymbol{R}_i|). \quad (13)$$

Eqn. (9) (subject to appropriate boundary conditions, as we will see below) deals with the effective Coulomb potential due to the electron distribution in the super-sphere of effective radius R. To solve it we exploit the fact that eqn. (9) separates in spherical polar coordinates r,θ,φ. The solution of Poisson's equation, eqn. (9), is given by

$$V_1(r,\theta,\varphi) = \sum_{l,m} F_{lm}(r)\,Y_{lm}(\theta,\varphi). \quad (14)$$

Each $F_{lm}(l\neq 0)$ satisfies the radial equation

$$\frac{1}{r}\frac{\mathrm{d}^2}{\mathrm{d}r^2}(rF) - \frac{l(l+1)}{r^2}F = -q_0^2 F. \quad (15)$$

Strictly, terms corresponding to $l=0$ have been considered separately

$$\frac{1}{r}\frac{\mathrm{d}^2}{\mathrm{d}r^2}(rF_{00}) - \frac{l(l+1)}{r^2}F_{00} = 4\pi\rho_0 - q_0^2 F_{00}.$$

The general solution for the radial equation is

$$F_{lm}(r) = \frac{(4\pi)^{3/2}}{q_0^2}\rho_0 + \frac{A_{00}}{r}\sin(q_0 r) + \frac{B_{00}}{r}\cos(q_0 r) + \sum_{j=0}^{l}\frac{C_{lj}}{q_0^j r^{j+1}}[B_{lm}\exp(-q_0 r) + (-1)^j A_{lm}\exp(q_0 r)], \quad (16)$$

where

$$C_{lj} = \frac{l(l+1)(l+j)!}{2^j j!(l-j)!}, \quad (17)$$

and A_{00}, B_{00}, A_{lm} and B_{lm} are constants that will be determined. The effective Coulomb potential V_1 can be written then as

$$V_1 = \frac{4\pi}{q_0^2}\rho_0 + \frac{A_{00}}{r}\sin(q_0 r) + \frac{B_{00}}{r}\cos(q_0 r) + \sum_{lm}{}'\sum_{j=0}^{l}\frac{C_{lj}}{q_0^j r^{j+1}} \times [B_{lm}\exp(-q_0 r) + (-1)^j A_{lm}\exp(q_0 r)]\; Y_{lm}(\theta,\varphi), \quad (18)$$

where the prime in the right hand term of the equation means that the summation over l begins from $l=1$. This potential has to be finite for $r=0$, which means that $B_{00}=0$, and $B_{lm} = (-1)^{l+1}A_{lm}$.

Taking eqn. (12) into account, we find the total effective Coulomb potential inside the super-sphere is

$$V_{\mathrm{in}} = \frac{4\pi}{q_0^2}\rho_0 + \frac{A_{00}}{r}\sin(q_0 r) + V_2(\boldsymbol{r}) + \sum_{lm}{}'\sum_{j=0}^{l}\frac{C_{lj}(-1)^j}{q_0^j r^{j+1}} \times A_{lm}[\exp(q_0 r) + (-1)^{1-j}\exp(-q_0 r)]\; Y_{lm}(\theta,\varphi), \quad (19)$$

everywhere except for $\boldsymbol{r}=\boldsymbol{R}_i$. Outside the super-sphere, a Laplace equation applies and the solution vanishing at infinity is

$$V_{\mathrm{out}} = \frac{B_{00}}{r} + \sum_{lm}{}'\frac{B_{lm}}{r^{l+1}}\,Y_{lm}(\theta,\varphi). \quad (20)$$

If the potential is specified on the surface of the bounding sphere, the coefficients entering eqns. (18) and (19) can be determined by evaluating $V(R,\theta,\varphi)$ and using

$$A_{lm} = \int \mathrm{d}\Omega\; Y_{lm}^*(\theta,\varphi)g(\theta,\varphi), \quad (21)$$

where $g(\theta,\varphi)$ is an arbitrary function. Here, g represents a "pseudo-charge density" designed to be a smooth, nodeless function which, in order to maintain the electrical neutrality

of the entire system, has to agree exactly with the true charge density outside the region bounded by the super-sphere of radius R.

An additional comment is appropriate here regarding the present theory. We begin by asking,"How unique is the potential in eqns. (18) and (19)?" If we demand that our "pseudo-charge density" g agree with the true charge density outside the "super-sphere" then the potential is uniquely determined. The inside region is not uniquely fixed by this procedure; however, if we require that the total charge of the valence electrons be normalized, then the fraction of electronic charge contained in this region must be large, *e.g.*, more than ~95% of the total. This means that the behavior of the charge contained in this region must dominate the static properties of the metallic cluster.

The effective cluster potential given by eqn. (18) displays the usual collective aspects of the electron gas. The primary manifestations of the collective behavior are (a) collective oscillations of the valence electrons as an entity, the so-called "plasma" oscillations, and (b) the screening of the field of any individual electric charge beyond a characteristic length q_0^{-1}. The former is fundamentally a diffraction effect, the electron wave nature being essentially disregarded in this kind of calculation. The screening of the ionic fields causes the remainder of the electron gas to stay diffuse, and so leads to a deficiency of negative charge just outside the immediate neighborhood of each positive ion enclosed in its neutralizing, co-moving electronic cloud. Thus the cluster potential exhibits additional spatial oscillations which are not determined solely by its behavior in the neighborhood of the electron at $\boldsymbol{r}$. In a collective oscillation, each individual electron suffers a small periodic perturbation of its velocity (recall that the electron density eqn. (5) is a result of the perturbation of the kinetic operator) and position due to the combined potential of all the other particles, both positive and negative. The cumulative potential of all the electrons may be quite large since the long range of the Coulomb interaction permits all the electrons to contribute to the potential at every point. This is, of course, partially balanced by the potential of the positive nuclei.) The collective behavior of the electron gas dominates phenomena involving distances greater than the characteristic length q_0^{-1}, while the individual particle component is associated with the random thermal motion of the electrons. In the approximate level of this analysis, the effects of collective excitation on the correlation are neglected, as a second-order effect.

Usually, the long range of the Coulomb interactions having the character of eqn. (18) precludes immediate application of these results to the calculation of the ground-state energy of the cluster. Therefore, we are not able to perform a minimization of the ground-state energy with respect to the volume of the super-sphere. Consequently, the self-consistency of the potential is affected by this lack of information.

With all the assumptions of the model and its mathematical output now presented, we may already point out some general characteristics we may expect for the behavior of the effective cluster potential. Since in the present perturbation approach the expansion of the electron density is based on plane waves, the cluster potential displays a high value in the central region. The potential is strongly dependent on the Coulomb correlations and, naturally enough, very sensitive to the position of the positive ions. (We discuss this aspect later.) Nonlocal effects due to the particle spins in the mean field for electrons are disregarded. Hence the method produces state-independent potentials.

In the following discussion, we work out an example of a metallic cluster M_{13} with icosahedral symmetry that closely approximates spherical symmetry. The model for the ionic cores is that of hard-spheres occupying a total volume in space equal to Ω_{ions}. The valence electrons are highly confined between the ionic cores. The unperturbed density ρ_0 is expressed by

$$\rho_0 = \frac{3}{4\pi r_s} = \frac{N}{\frac{4\pi}{3}R^3 - \Omega_{\text{ions}}}, \tag{22}$$

where r_s is a point in the space available to the electrons, the "electronic interspace", outside the ion cores. This means that we have subtracted from the entire volume of the super-sphere of radius R the volume assigned to the ionic cores Ω_{ions}; N is the total number of the delocalized electrons, equal to the number of ionic charges. The distance between the centers of the central and outer ions is the bond length. For numerical calculation we set $R_i = 5.9\ a_0$. The core volume Ω_{ions} is usually computed by taking into account the ionic radius. In the following, we let this radius be 2.74 a_0 so the resulting volume Ω_{ions} is 1122 $(a_0)^3$. For this first example, the electronic interspace was chosen to be in $r_s = 0.75\ a_0$, in accordance with the high-density electron gas requirement ($r_s \ll 1$), and by imposing that 95% of the total electrons must be inside the super-sphere, the super-sphere radius becomes $R = 6.5\ a_0$. In Fig. 1 we can see the corresponding effective potential inside the super-sphere as a function of r and θ. In Fig. 2, the spatial dependence of the same potential is displayed along the coordinates θ and ϕ at the radius where the outer ions lie, $R_i = 5.9\ a_0$. These pictures show the regular, collective characteristics we discussed above. The oscillations we observe are a

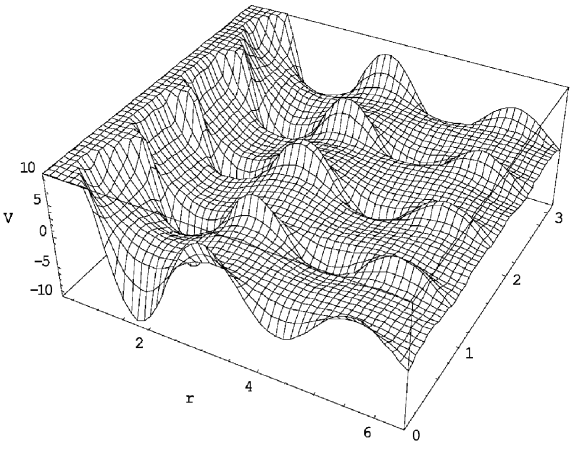

Fig. 1 The effective electrostatic potential inside the cluster cage for M_{13} for $0 < r < 6.5\ a_0$, $0 < \theta < \pi$ rad and $\varphi = 0$.

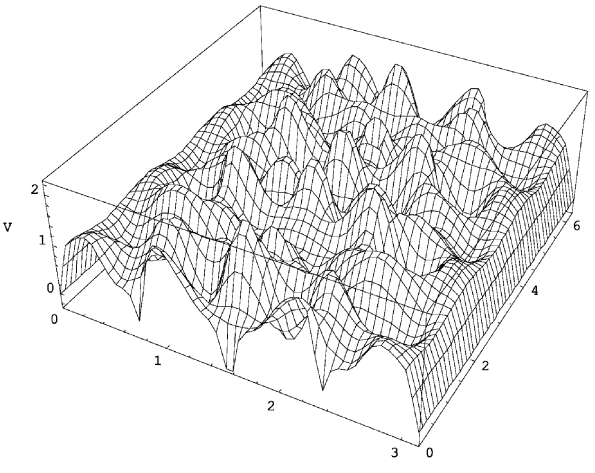

Fig. 2 The same effective electrostatic potential displayed as a $\theta - \varphi$ plot at the position of the surface ions.

manifestation of the self-consistency of Poisson's equation and represent the main correlation effect of the electron gas in the metallic state (the high-density limit).

Despite the collective aspects which contribute to the mean-field character of the effective potential, $V(\boldsymbol{r})$ remains sensitive to the geometry and composition of the cluster. If, for example, one host atom in the cluster cage is replaced by an impurity atom A, the potential reflects this structural change. We explore this property in the following. Let us assume that the impurity A is a trivalent metal atom which releases all three of its valence electrons into the Fermi sea in the bulk volume. We take its core volume to be the same as the M ions. With the foreign atom at the center of the cluster, the substitution does not change the symmetry; we assume that the most stable geometry of the cluster does have the dopant at the centre. Figs. 3 and 4 show the corresponding effective electrostatic potential for the AM_{12} system. By comparing this with the effective mean-field potential for M_{13}, we observe that the presence of the trivalent atom at the center makes the potential much deeper. The first minimum along the r coordinate is about twice as deep (from -5 au to -10 au) as that corresponding to the homogeneous cluster, in above. (See Fig. 3, where V is displayed as a function of r and θ.) The delocalized electrons polarize inward, toward the high Coulomb field of the central, trivalent ion. Fig. 4 shows also that the shape of the quantum oscillations at the cluster surface changes relative to the previous case. The amplitudes of oscillations become rather uniform which means that the screening among the electric charges is much better for this system than for the homogeneous cluster, a consequence of the increased number of delocalized electrons, from 13 to 15. Moreover the better screening effect here results in a change in the effective force acting in the electron gas. This can be seen in Fig. 4 as a phase-shift of electron density oscillations at the position of certain positive ions. (Compare this with the effective potential displayed in Fig. 2.)

If we move the trivalent ion to the outer shell, the disturbance of course goes toward the surface and the electron density is enhanced around the vertex where the trivalent ion is located. (See Fig. 5 and guide the eye along the r coordinate, from the origin towards the position of the trivalent impurity of coordinates $r = 5.9$, $\theta = 0$.) This behavior of the effective potential is supplemented by the appearance of more pronounced Coulombic correlations of the valence electrons near the trivalent impurity. The quantum oscillations are sensibly disturbed by the trivalent impurity located on the cluster surface. This disturbance appears as irregular behavior along the θ coordinate at constant r. Also, a large potential difference, about 1 au, can be seen in Fig. 6 between the position

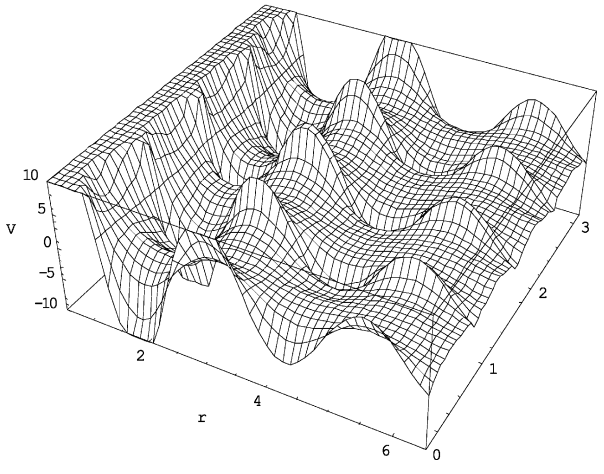

Fig. 3 The corresponding effective electrostatic potential for AM_{12} system for $0 < r < 6.5\ a_0$, $0 < \theta < \pi$ rad and $\varphi = 0$ with the impurity in the center of the icosahedral cluster cage.

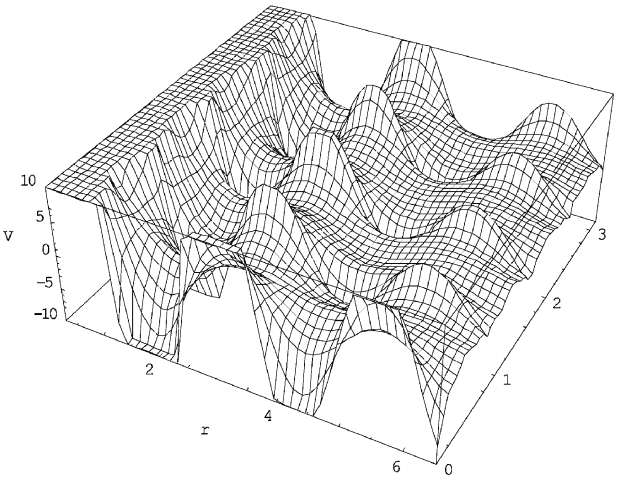

Fig. 5 A plot analogous to that of Fig. 3, for the AM_{12} system with impurity at the vertex, ($\theta = 0$, $\varphi = 0$) and for $0 < r < 6.5\ a_0$.

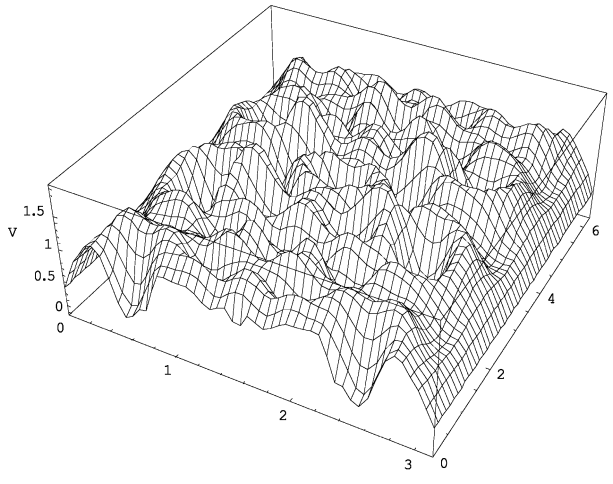

Fig. 4 The effective electrostatic potential showed in Fig. 3 displayed here along the coordinates θ and φ at the position of surface ions.

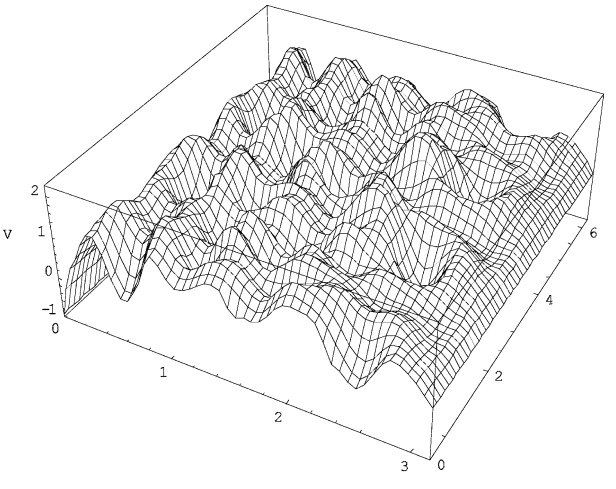

Fig. 6 The $\theta - \varphi$ spatial dependence of the potential displayed in Fig. 5 at the position of the outermost ion shell.

of the trivalent impurity ($\theta = 0$, $\varphi = 0$) and the antipodal position ($\theta = \pi$, $\varphi = 0$) occupied by a host ion. The potential difference leads to a displacement of the electronic cloud towards the position of the trivalent ion and a deficiency of negative charge in the opposite direction. Consequently, a diffusive trend of electron density oscillations can be observed in the hemisphere at $\theta = \pi$.

We may conclude that the effective electrostatic potentials for metallic clusters are subject to important Coulombic correlation effects that can be visualized at the proper scale by employing a discrete description for the positive background. The electron density shows a static screening which is rather localized near the positive charges and supplemented by the long-range oscillatory behavior. For singly-doped binary metallic systems, the depth of the effective electrostatic potential depends on the dopant position in the cluster geometry. The collective aspects of the excitations of electrons delocalized through the cluster volume are strongly perturbed by the presence of the impurity. The main effect of these structural rearrangements of the ions is the change of the effective potential, as we have shown. The change of the cluster potential may, in turn, alter the ordering of the related electron shells, a fact which has been observed in many experiments.[30–32] Therefore our findings may be interpreted as qualitative support for various models explaining the shell inversions for doped metallic clusters.[38–41] Obviously other kinds of changes of dopant atoms may induce still different effects, that will depend on their locations in the cluster.

Finally, we may say that the method developed here is simple and flexible and can yield, to some extent, accurate approximations to the exact effective potentials with minor computing effort. Also, it has the advantage of physical immediacy, *i.e.*, the present approach is easy to interpret. This makes the method useful for a fast check of the effective potential to systems, clusters of heavy elements, for example, presently beyond the capability of more accurate approaches.

Acknowledgement

This research was supported by a Grant from the National Science Foundation.

References

1 M. Brack, *Rev. Mod. Phys.*, 1993, **65**, 677.
2 *Theory of the Inhomogeneous Electron Gas*, ed. S. Lundqvist and N. H. March, Plenum, New York, 1983.
3 I. Lindgren and S. Lundqvist, *Nobel Symposium*, Göteborg, 1980.
4 The main tools employed here are the first-and second-order density matrices, N. H. March, W. H. Young, and S. Sampanthar, in *The Many-Body Problem in Quantum Mechanics*, Dover, New York, 1995, which allow an analytical derivation of the electron density, N. H. March, R. Pucci, *J. Chem. Phys.*, 1982, **75**, 497; K. A. Dawson and N. H. March, *Phys. Lett. A*, 1983, **94**, 434; G. Senatore and N. H. March, *Rev. Mod. Phys.*, 1994, **66**, 445, and Green's function, largely used in quantum computer simulations, N. H. March and M. Parrinello, in *Collective Effects in Solids and Liquids*, Adam Hilger, Bristol, 1982G. D. Mahan, in *Collective Many-Particle Physics*, Plenum, New York, 2nd edn., 1990S. Wilson, in *Electron Correlation in Molecules*, University Press, Oxford, 1988.
5 P. Rehmus, M. E. Kellman and R. S. Berry, *Chem. Phys.*, 1978, **31**, 239.
6 P. Rehmus and R. S. Berry, *Chem. Phys.*, 1979, **38**, 257; P. Rehmus, C. C. J. Roothaan and R. S. Berry, *Chem. Phys. Lett.*, 1978, **58**, 321.
7 See, for review, R. S. Berry, in *The Lesson of Quantum Theory*, ed. J. deBoer and O. Ulfbeck, North-Holland, Amsterdam, 1986, p. 241; R. S. Berry, *Contemp. Phys.*, 1989, **39**, 1; R. S. Berry and J. Krause, *Adv. Chem. Phys.*, 1988, **70**(1), 35R. S. Berry, in *Structure and Dynamics of Atoms and Molecules*, ed. J. L. Calais and E. S. Kryachko, Kluwer, Dordrecht, 1995, p. 155.
8 S. Chandrasekhar, *Sci. Mon.*, 1947, **64**.
9 C. A. Coulson and A. H. Neilson, *Proc. Phys. Soc. London, Ser. A*, 1951, **78**, 831.
10 P. G. Dickens and J. W. Linnett, *Quart. Rev.*, 1957, **11**, 291.
11 O. Sinanoglu and K. A. Brueckner, *J. Am. Chem. Soc.*, 1970, **88**, 13.
12 H. Wulfman and S. Kumei, *Phys. Rev. A*, 1973, **9**, 2306.
13 D. R. Herrick and O. Sinanoglu, *Phys. Rev. A*, 1975, **11**, 97.
14 K. E. Banyard and D. J. Ellis, *J. Phys. B*, 1975, **8**, 2311.
15 U. Fano, *Phys. Today*, 1976, **29**, 32.
16 K. E. Banyard and J. Sanders, *J. Chem. Phys.*, 1994, **101**, 3096.
17 N. H. March and R. Pucci, *J. Chem. Phys.*, 1982, **75**, 497; K. A. Dawson and N. H. March, *Phys. Lett. A*, 1983, **94**, 434; G. Senatore and N. H. March, *Rev. Mod. Phys.*, 1994, **66**, 445N. H. March and M. Parrinello, in *Collective Effects in Solids and Liquids*, Adam Hilger, Bristol, 1982G. D. Mahan, in *Collective Many-Particle Physics*, Plenum, New York, 2nd edn., 1990S. Wilson, in *Electron Correlation in Molecules* Oxford University Press, Oxford, 1988.
18 N. H. March, *Phys. Lett. A*, 1985, **84**, 319; N. H. March, *Phys. Lett. A*, 1985, **113**, 66.
19 G. Senatore and N. H. March, *J. Chem. Phys.*, 1985, **83**, 1232.
20 D. Herschbach, *J. Chem. Phys.*, 1986, **84**, 838.
21 T. Schork and P. Fulde, *J. Chem. Phys.*, 1992, **97**, 9195.
22 K. Jankowski and P. Malinowski, *Int. J. Quantum Chem.*, 1993, **48**, 59.
23 R. J. Bartlett, *Annu. Rev. Phys. Chem.*, 1981, **32**, 359; R. J. Bartlett, *Annu. Rev. Phys. Chem.*, 1989, **93**, 1697.
24 N. H. March and M. Parrinello, in *Collective Effects in Solids and Liquids* Adam Hilger, Bristol, 1982.
25 G. D. Mahan, in *Collective Many-Particle Physics*, Plenum, New York, 2nd edn., 1990.
26 S. Wilson, in *Electron Correlation in Molecules*, Oxford University Press, Oxford, 1988.
27 J. Friedel, *Philos. Mag.*, 1952, **43**, 153.
28 N. H. March, W. H. Young and S. Sampanthar, in *The Many-Body Problem in Quantum Mechanics*, Dover, New York, 1995.
29 "Semiclassical" denotes here the situation with sufficiently slowly varying potential. It is worth-while mentioning here that a similar method was first applied by Kohn and Sham to describe a system of electrons subject to a very slowly varying external potential, W. Kohn and L. J. Sham, *Phys. Rev.*, 1965, **137**, 1697.
30 M. Heinebrodt, N. Malinowski, F. Tast, W. Branz, I. M. L. Billas and T. P. Martin, *J. Chem. Phys.*, 1999, **110**, 9915.
31 W. Bouwen, F. Vanhoutte, F. Despa, S. Bouckaert, S. Neukermans, L. Theil Kuhn, H. Weidele, P. Lievens and R. E. Silverans, *Chem. Phys. Lett.*, 1999, **314**, 227.
32 J. Akola, M. Manninen, H. Hakkinen, U. Landman, X. Li and L. S. Wang, *Phys. Rev. B*, 1999, **60**, 11 297.
33 This makes the connection between March's theory of perturbed electron density, N. H. March and A. M. Murray, *Phys. Rev.*, 1960, **120**, 830, and Mott's treatment of imperfections in metals, N. F. Mott, *Proc. Cambridge Philos. Soc.*, 1936, **32**, 281.
34 F. Despa, *Phys. Rev. B*, 1998, **57**, 7335.
35 To remove this qualitative defect, we should work with the electron density within primary form, eqn. (5), which remains finite at the origin for a potential which is singular as r^{-1}. Further employment of eqn. (6) for the electron density has the advantage of producing an analytical result for the effective cluster potential.
36 There exists a limit within which we can regard the Fermi fluid as a high density gas. Accordingly, the electron wave vector must be larger than $k_c \sim 0.68\ k_F$, where k_F is the Fermi wave vector. The above result was obtained by a minimizing procedure of the lowest state energy, see D. Pines, *Phys. Rev.*, 1953, **92**, 626; D. Bohm and D. Pines, *Phys. Rev.*, 1953, **92**, 609. According to the above criterion, the region of high kinetic energy of the electron (and therefore, rapidly varying wave functions) is consistent with the high density approximation.
37 M. L. Cohen, M. Schlüter, J. R. Celikowsky and S. G. Louie, *Phys. Rev. B*, 1975, **12**, 5575; J. R. Chelikowsky, *Phys. Rev. B*, 1980, **21**, 3074.
38 M. M. Kappes, P. Radi, M. Schär and E. Schumacher, *Chem. Phys. Lett.*, 1985, **119**, 11.
39 C. Yeretzian, *J. Chem. Phys.*, 1995, **99**, 123.
40 C. Baladron and J. A. Alonso, *Phys. Lett. A*, 1989, **140**, 67.
41 C. Yannouleas, P. Jena and S. N. Khanna, *Phys. Rev. B*, 1992, **46**, 9751.